

TEXTURE GROWTH CHARACTERIZATION IN RARE EARTH HYDROGEN STORAGE ALLOYS^①

Wang Chaoqun, Wang Ning, Jin Hongmei and Li Guoxun

General Research Institute for Nonferrous Metals, Beijing 100088, P. R. China

ABSTRACT By using X-ray diffraction technique and electrochemical measurements, the texture growth and its effects on the electrochemical properties have been explored under various cooling rates in rare-earth hydrogen storage alloys. It was shown that: (1) the different texture growth characters were obtained in the rare earth hydrogen storage alloys with various compositions under conventional fast cooling and a columnar structure was formed so that the *c*-axis of the hexagonal structure was oriented parallel to the cooling plane and a higher capacity was attained; (2) the alloy prepared from rapid solidification exhibits a strong (0002) based pole texture in the surface of alloy sheet, i.e. *c*-axis texture. Its crystal growth character is consistent well with the alloy $MmNi_{3.5}Co_{0.7}Al_{0.8}$ which has a columnar structure with very high endurance, and low lattice strain was obtained under controlled conditions including high rate cooling in the casting process for obtaining a columnar structure.

Key words rare earth hydrogen storage alloy texture rapid solidification capacity cycle life

1 INTRODUCTION

Ni/MH rechargeable batteries using hydrogen storage alloys have received great attention because of high capacity, no Cd contamination, memory-free effect and very high endurance. A large amount of research work was concerned with the alloy preparation technology and its properties, but only a few works about texture growth of the hydrogen storage alloys were reported. Sakai *et al*^[1] reported for the first time that a columnar structure was formed so that the *c*-axis of the hexagonal structure was oriented parallel to the cooling plane in the as-cast $MmNi_{3.5}Co_{0.7}Al_{0.8}$ alloy under controlled conditions including high rate cooling in the casting process. The as-cast alloy with only the columnar structure exhibits homogeneous composition and low lattice strain without heat treatment. It was also observed for the as-cast alloy electrode that the X-ray diffraction peaks at large angles become sharper after charge-discharge cycles showing that release of lattice strain, i.e. "hydrogen induced homogenization", thus enhancing the stability and cycle life of the Ni/MH alkaline secondary battery. In addition, some researchers^[2-5] had also studied the influence of the microstructures of rapidly solidified AB₅ type alloys on the diffusion of hydrogen atoms and the properties of metal hydride electrode. It is found that there is a critical growth rate for the cellular-dendritic structure transition and columnar grain growth preferentially in the direction perpendicular to the *c*-axis of the hexagonal CaCu₅ type structure, leading to the low lattice strain and high resistance to pulverization of the alloy^[2-6]. The preferential growth crystal planes are transformed from {110} into {200}, in effect, it is rotated about 30° around the *c*-axis of hexagonal AB₅ type structure, leading to the high-rate discharge efficiency of the electrode. It may be seen that the rapidly solidified LaNi₅-based hydrogen storage alloys could be prepared with columnar structure and preferential crystal growth *c*-axis orientation. Therefore the development of the rapid cooling technology for the

drogen induced homogenization", thus enhancing the stability and cycle life of the Ni/MH alkaline secondary battery. In addition, some researchers^[2-5] had also studied the influence of the microstructures of rapidly solidified AB₅ type alloys on the diffusion of hydrogen atoms and the properties of metal hydride electrode. It is found that there is a critical growth rate for the cellular-dendritic structure transition and columnar grain growth preferentially in the direction perpendicular to the *c*-axis of the hexagonal CaCu₅ type structure, leading to the low lattice strain and high resistance to pulverization of the alloy^[2-6]. The preferential growth crystal planes are transformed from {110} into {200}, in effect, it is rotated about 30° around the *c*-axis of hexagonal AB₅ type structure, leading to the high-rate discharge efficiency of the electrode. It may be seen that the rapidly solidified LaNi₅-based hydrogen storage alloys could be prepared with columnar structure and preferential crystal growth *c*-axis orientation. Therefore the development of the rapid cooling technology for the

① Project 59872006 supported by the National Natural Science Foundation of China

Received Mar. 27, 1998; accepted Dec. 4, 1998

rare earth hydrogen storage alloy is another way to enhance the comprehensive properties of the alloy electrodes. By using the X-ray diffraction and electrochemical measurements, the texture growth character and its effects on the electrochemical properties have been explored under controlled conditions, including high rate cooling in the casting process for obtaining a columnar structure, rapid solidification and prevention of stoichiometric deviation in this paper.

2 EXPERIMENTAL

AB₅-type rare earth hydrogen storage alloys La_xNd_yPr_{1-x-y}B₅ and La_xNd_yCe_zPr_{1-x-y-z}B₅ (B represents Ni, Co, Mn, Al) were prepared as buttons by mixing appropriate amounts of metals with a purity higher than 99.9% (mass fraction), and arc melting the mixtures under a purified argon atmosphere. The buttons were remelted 2 or 3 times to ensure homogeneity and then cast in a water-cooled copper crucible. Rapidly solidified samples were produced by using a melt-spinning technology. The alloy specimens were pulverized mechanically below 300 mesh, the alloy powder mixed with fine copper powder in the respective mass ratio of 1:4 was pressed into a pellet electrode of $d = 13 \text{ mm} \times 1.1 \text{ mm}$ at a pressure of 30 MPa^[8]. A glass cell with three compartments was employed for electrochemical measurements. The electrolyte is a 6 mol/L KOH solution. A Hg/HgO (6 mol/L KOH) reference electrode was positioned closely to the electrode in the working electrode compartment. For discharge capacity measurements, the negative electrode was charged for 2 h at 200 mA/g and discharged to -0.65 V at 100 mA/g against Hg/HgO electrode. For cycle life experiments the negative electrode was charged for 2.33 h at 150 mA/g and discharged at a current of 150 mA/g to 0.9 V.

The alloy ingots were mechanically cut into two sections (i.e. parallel and perpendicular to the columnar structure), and then by using X-ray diffraction technique to determine the phase constituents and the intensities of all peaks in the hydrogen storage alloys so as to attain the inverse pole figures. The X-ray diffraction mea-

surements were carried out on APD-10 diffractometer with CuK_α, graphite monochromator, scanning speed 1 (°)/min, and measured range from 20° to 75° (2θ). The pole densities of the inverse pole figures for rapidly solidified samples were calculated by

$$P_{hkl} = \frac{I_{hkl}^t / I_{hkl}^r}{\sum A_{hkl} \cdot I_{hkl}^t / I_{hkl}^r} \quad (1)$$

where I_{hkl}^t and I_{hkl}^r represent textured and random intensities respectively, A_{hkl} are area weight coefficients, and P_{hkl} are pole densities of (hkl) planes^[7].

3 RESULTS AND DISCUSSION

The cast ingot shows a macrostructure consisting of a columnar structure in the outer region and an equiaxial structure in the inner region. A higher cooling rate (by pouring the melted alloy into a water-cooled mould) results in an ingot with only columnar structure. The sample prepared by arc melting exhibits smooth and densified columnar structure, while the grain boundaries are clear^[9].

Table 1 lists the texture analysis results of the columnar structure of parallel and vertical sections in the La_xNd_yPr_{1-x-y}B₅ alloy ingots. Table 2 lists the preferential crystal growth in La_xNd_yCe_zPr_{1-x-y-z}B₅ alloy ingots. It can be seen that the mainly preferential orientation planes of the V-type texture (i.e. perpendicular to columnar structure) are {110} + {200}, while those of the P-type texture (i.e. parallel to columnar structure) are {101} + {002} + {201}. The preferential orientation planes depend on the alloy composition, but columnar grains grow preferentially in the direction perpendicular to the c-axis of the hexagonal CaCu₅-type structure, leading to lattice strain and high resistance to pulverization of the alloy. It is consistent well with the results of c-axis texture about the columnar structure in the rapidly cooled Mm-Ni_{3.5}Co_{0.7}Al_{0.8} hydrogen storage alloy^[11]. In the meanwhile the results also correspond to the unidirectionally solidified microstructure and its preferential orientation planes change from {110} to {200} at different cooling rates^[5], i.e.

the preferential crystal planes rotate about 30° around the c -axis. The high-rate discharge capability of unidirectionally solidified hydrogen storage alloy is associated with the anisotropic crystal growth. This might be attributed to the fact that the unidirectionally solidified alloy has better homogeneity and crystallinity, and the preferential precipitation of Ni and Co on the grain boundaries, which could improve the electrocatalytic activity of the alloy surface^[6]. It has been shown that there are three main crystallographic features in the rapidly solidified R. E. based hydrogen storage alloy, i.e. preferential grain growth, anisotropically deformed crystal lattices (decreased a -axis and increased c -axis), and the change in atomic order. The (0002) based pole texture is essential, and its inverse pole figure is shown in Fig.1. The pole densities of rapidly solidified sample and its annealing samples (at 400, 600, and 800 °C) are given in Table 3. It can be seen that the (0002) based pole texture is formed on the alloy surface and the dendritic columnar grains also grow preferentially in the direction perpendicular to the c -axis of the hexagonal CaCu_5 -type structure.

From the above texture analyses and the discharge capacity measurement, it follows that the alloy having (101) + (002) planes parallel to columnar structure shows high capacity and endurance. Fig.2 shows the active process of the rapidly cooled alloys. It can be seen that, most alloys were activated in the first few charge-discharge cycles, and some alloys seem to be easily activated (only after two or three cycles). Fig.3 shows the relationship between the dis-

charge capacity and high rate discharge current. From the slopes of the curves we can see that No.7, 13 and 15 alloys show smoother slopes, even though their discharge capacities do not reach the maximum value. In addition, No.11 and 15 alloys have relatively good cycle lives (with low rate decays capacity of 16% and 18% after 300 cycles). The alloys with relatively good high rate dischargeabilities were observed with {201} + {101} type preferential orientation planes in parallel to the columnar structure. However, up to now there are not any reports to clarify how the texture affects the electrochemical properties of the hydrogen storage alloy electrode yet. Based on the above results it seems to draw a conclusion that the c -axis texture formed in the direction perpendicular to the solidified microstructure associated with grain size reduction and hence the columnar dendritic microstructure could be crushed into a fine grain size during the initial step at the hydrogen acti-

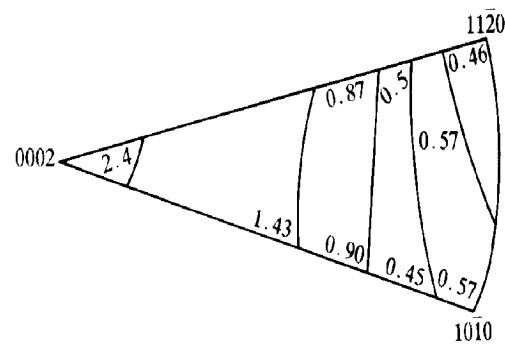


Fig.1 Inverse pole figure of rapidly solidified R. E. hydrogen storage alloy

Fig.2 Dependence of discharge capacity on charge-discharge cycles in No.1 ~ No.16 alloys

Table 1 Texture growth character and discharge capacity of $La_xNd_yPr_{1-x-y}(NiCoMnAl)_5$ alloy ingot

| Sample No. | Composition of A side in AB_5 | | | Value of A | Texture oriented planes (hkl) | | Discharge capacity / ($mAh \cdot g^{-1}$) |
|------------|---------------------------------|------|------|------------|-----------------------------------|--------------------------------|---|
| | La | Nd | Pr | | Vertical to columnar structure | Parallel to columnar structure | |
| 1 | 0.65 | 0.10 | 0.05 | 0.80 | (110) + (200) | (301) + (101) | 288 |
| 2 | 0.65 | 0.05 | 0.20 | 0.90 | (110) + (200) | (101) + (201) | 300 |
| 3 | 0.85 | 0.20 | 0.20 | 1.25 | (301) + (111) | (201) + (101) | 291 |
| 4 | 0.85 | 0.05 | 0.05 | 0.95 | (110) + (112) | (002) + (101) + (211) | 306 |
| 5 | 0.75 | 0.10 | 0.15 | 1.00 | (110) + (200) | (201) + (211) | 261 |
| 6 | 0.75 | 0.20 | 0.15 | 1.15 | (200) + (110) | (201) | 273 |

Table 2 Texture growth character and discharge capacity of $La_xNd_yCe_zPr_{1-x-y-z}(NiCoMnAl)$ alloy ingot

| Sample No. | Composition of A side in AB_5 | | | | Value of A | Texture oriented planes (hkl) | | Discharge capacity / ($mAh \cdot g^{-1}$) |
|------------|---------------------------------|------|------|------|------------|-----------------------------------|--------------------------------|---|
| | La | Nd | Ce | Pr | | Vertical to columnar structure | Parallel to columnar structure | |
| 1 | 0.40 | 0.15 | 0.50 | 0.05 | 1.10 | (201) + (110) | (101) + (201) | 322 |
| 2 | 0.40 | 0.35 | 0.05 | 0.10 | 0.90 | (200) + (112) | (101) + (201) | 318 |
| 3 | 0.40 | 0.05 | 0.35 | 0.20 | 1.00 | (110) + (301) | (101) + (002) + (201) | 312 |
| 4 | 0.40 | 0.25 | 0.20 | 0.15 | 1.00 | Random | (301) + (201) + (101) | 295 |
| 5 | 0.50 | 0.05 | 0.50 | 0.10 | 1.15 | (110) + (200) | (101) | 326 |
| 6 | 0.50 | 0.25 | 0.05 | 0.05 | 0.85 | (110) + (301) | (101) + (111) | 312 |
| 7 | 0.50 | 0.15 | 0.35 | 0.15 | 1.15 | (200) + (110) | (211) + (101) | 286 |
| 8 | 0.50 | 0.35 | 0.20 | 0.20 | 1.25 | (111) | (211) + (101) | 283 |
| 9 | 0.70 | 0.25 | 0.05 | 0.20 | 1.20 | (111) + (301) | (101) + (201) | 311 |
| 10 | 0.70 | 0.05 | 0.05 | 0.15 | 0.95 | (200) + (111) | (112) | 302 |
| 11 | 0.70 | 0.35 | 0.05 | 0.05 | 1.15 | (110) + (200) | (211) + (101) + (002) | 289 |
| 12 | 0.70 | 0.05 | 0.20 | 0.10 | 1.05 | (200) + (110) | (101) + (201) | 296 |
| 13 | 0.60 | 0.35 | 0.05 | 0.15 | 1.15 | (200) + (110) | (101) + (201) + (301) | 305 |
| 14 | 0.60 | 0.15 | 0.05 | 0.20 | 1.00 | (110) + (200) | (101) + (201) + (112) | 291 |
| 15 | 0.60 | 0.25 | 0.05 | 0.10 | 1.00 | (110) + (200) | (002) + (301) + (101) | 300 |
| 16 | 0.60 | 0.05 | 0.20 | 0.05 | 0.90 | (200) + (110) | (101) + (201) | 311 |

vation. Because of the refined grain size a large amount of grain boundaries could provide diffusion paths for the hydrogen during the charge-discharge process, thus releasing the lattice strain (hydrogen induced homogenization). The high rate discharge efficiencies of the electrodes depend mainly on the diffusion kinetics of hydrogen atoms in the alloys and electrocatalytic activities on the electrode surface^[5]. Among the others the anisotropically preferential grain growth

also led to higher electrocatalytic activity due to the anisotropic diffusion of hydrogen on some crystallographic planes. The detailed mechanism remains to be further clarified.

4 CONCLUSIONS

The different texture growth characters were observed in rare earth based hydrogen storage alloys with various compositions under con-

Fig. 3 Dependence of discharge capacity on high-rate discharge current in No.1 ~ No.16 alloys**Table 3** Pole density of inverse pole figure on surface in rapidly solidified alloy

| (hkl) | P_{hkl} | | | |
|-------|----------------------|------------------|------------------|------------------|
| | Rapid solidification | 400 °C annealing | 600 °C annealing | 800 °C annealing |
| 001 | 2.40 | 2.27 | 2.43 | 2.36 |
| 101 | 0.90 | 0.99 | 1.03 | 1.05 |
| 110 | 0.46 | 0.57 | 0.51 | 0.60 |
| 200 | 0.57 | 0.49 | 0.52 | 0.50 |
| 111 | 0.50 | 0.64 | 0.63 | 0.67 |
| 002 | 2.40 | 2.25 | 2.64 | 2.34 |
| 201 | 0.45 | 0.39 | 0.50 | 0.40 |
| 112 | 0.87 | 1.01 | 0.88 | 1.06 |
| 211 | 0.57 | 0.64 | 0.54 | 0.68 |
| 202 | 0.70 | 0.78 | 0.75 | 0.81 |
| 300 | 0.57 | 0.49 | 0.52 | 0.50 |
| 103 | 1.43 | 1.47 | 1.38 | 1.53 |

ventional fast cooling, and a columnar structure was formed so that the c -axis of the hexagonal CaCu_5 type structure was oriented parallel to the cooling plane. It was observed that there are preferential orientation planes $\{110\} + \{200\}$ in the direction vertical to the columnar structure and $\{101\} + \{002\}$ preferential orientation planes were formed in the direction parallel to the columnar structure. The unidirectionally solidified alloy with a similar preferential orientation feature, i.e. dendritic-columnar grains preferentially in the direction perpendicular to the c -

axis, but the preferred orientation plane rotated from $\{110\}$ to $\{200\}$ about 30° around the c -axis at different solidified rates. The rapidly solidified alloys exhibit mainly the $\{0002\}$ based pole textures on the alloy surface and the grains grow preferentially in the direction perpendicular to the c -axis of the hexagonal structure. The high rate discharge efficiency of the electrodes depends mainly on the preferential c -axis orientation growth and the anisotropic hydrogen diffusion.

REFERENCES

- 1 Sakai T, Yoshinaga H, Miyamura H *et al.* J Alloys Comp, 1992, 180: 37.
- 2 Sakai T, Hazama T, Miyamura H *et al.* J Alloys Comp, 1991, 172 - 174: 1175.
- 3 Tang W and Sun G. J Alloys Comp, 1994, 203: 195.
- 4 Mishima R, Miyamura R and Sakai H T. J Alloy Comp, 1993, 192: 176.
- 5 Luo Y, Kang L, Lei Y *et al.* Chinese J Power Sources, (in Chinese), 1997, 21(4): 147.
- 6 Jin H, Li G and Wen Z. Chinese Rare Metals, (in Chinese), 1997, 21: 173.
- 7 Lu X, Dai Q and Li D. Chinese Rare Metals, (in Chinese), 1996, 20: 410.
- 8 Wang C Q, Jin H, Li G *et al.* Chinese Metals Physics Exam and Test, 1998, (1): 20.
- 9 Wang C Q, Jin H, Li G *et al.* Chinese J Power Sources, (in Chinese), 1998, 22(1): 5.

(Edited by Peng Chaoqun)